Cellular Oncology 31 (2009) 357–370
DOI 10.3233/CLO-2009-0481
IOS Press

Multiple localization of endogenous MARK4L protein in human glioma

Ivana Magnani [a], Chiara Novielli [a], Melissa Bellini [a], Gaia Roversi [a], Lorenzo Bello [b] and Lidia Larizza [a,*]

[a] *Dipartimento di Medicina, Chirurgia e Odontoiatria, Sezione di Genetica Medica, Università di Milano, Milan, Italy*

[b] *Dipartimento di Scienze Neurologiche, Università di Milano, Milan, Italy*

Abstract. *Background*: We have previously shown that the sustained expression of MARK4L transcripts in glioma and neural progenitors (NHNPs) declines after exposure to antisense MARK4L oligonucleotides in glioblastoma cell lines. Array-CGH confirmed the genomic duplication of MARK4L identified by FISH in a glioblastoma cell line. This background together with literature data on the exogenous association of MARK4 with interphase centrosome prompted us to investigate the sub-cellular localization of the endogenous MARK4L protein aiming at achieving insights on its possible role in the pathomechanisms of glioma.

Methods: Immunodetection was carried out to validate the specificity of MARK4L antibody in gliomas and NHNPs. Mass spectrometry was applied for MARK4L protein identification in a representative glioblastoma cell line. Combined biochemical fractionation and immunodetection analyses were performed to confirm the sub-cellular localization of MARK4L achieved by immunofluorescence in glioma cell lines.

Results: By assigning MARK4L protein within the band immunoprecipitated by the specific antibody we validated our anti-MARK4L antibody. We demonstrated that the endogenous MARK4L: (i) colocalizes with centrosomes at all mitotic stages and resides in centrosome-enriched fractions; (ii) associates with the nucleolus and the midbody and respective fractions, and (iii) co-stains the aberrant centrosome configurations observed in glioma cell lines.

Conclusion: The overall data merge on the multiplex entry of MARK4L into the cell cycle and link it to the aberrant centrosomes in glioma cell lines suggesting a possible role of this kinase in the abnormal mitotic processes of human glioma.

Keywords: Glioma, MARK4L, immunodetection, multiple subcellular localization, centrosome abnormalities

1. Introduction

Microtubule affinity regulating kinases (MARKs) have attracted attention because of their ability to phosphorylate a serine motif that is critical for the microtubule binding of the neuronal microtubule-associated proteins (MAPs) tau and MAP2 in Alzheimer neurofibrillary degeneration [1]. A general role of the MARKs in regulating MAP interaction with microtubules can be inferred from the results of studies of MAP4 showing that the ubiquitous MAPs affect microtubule stability in dividing cells [2].

MARKs are regulated by a number of finely tuned mechanisms, including phosphorylation of the activation loop (T-loop) by MARKK/TAO-1 [3] and LKB1/Par-4 kinases [4], phosphorylation of the spacer domain by atypical PKC [5], and binding to the scaffolding proteins 14-3-3 [6] or PAK5, a neuronal member of the p21-activated kinases [7]. MARK4 is the least well known member of the family but, unlike the others, co-localizes with interphase centrosomes, microtubules, the cytoskeleton and neurite-like processes of neuroblastoma cells [8]. Furthermore, when transfected into HEK293 cells, it co-immunoprecipitates with tau, tubulin (α, β, γ), actin, myosin and hsp70 [8]. Taken together, these findings suggest a multifunctional role in both basic and cell-specific processes.

MARK4 transcripts are ubiquitously expressed, but the highest expression levels are found in brain and testis [9]. The two main RNA molecular species de-

*Corresponding author: Lidia Larizza, Dipartimento di Medicina, Chirurgia e Odontoiatria, Sezione di Genetica Medica, Università di Milano, Polo San Paolo, via di Rudinì, 8, 20142 Milan, Italy. Tel.: +39 02 50323206; Fax: +39 02 50323026; E-mail: lidia.larizza@unimi.it.

scribed so far are a result of the alternative splicing of exon 16 and lead to the MARK4L and MARK4S isoforms, which are differentially expressed in the central nervous system (CNS) [10–12]. The encoded proteins differ in the C-terminal region: the L isoform is characterized by the ELKL motif, whereas the S isoform has a unique domain with no homology to any known structure [13]. We have previously described the substantial transcript levels of MARK4L in gliomas and their decline after exposure to anti-sense MARK4L oligonucleotides [10].

Human gliomas are a heterogeneous group of astrocytomas, oligodendrogliomas and mixed oligoastrocytomas, and are graded as WHO II, III or IV. The most aggressive, grade IV astrocytoma, is referred to as glioblastoma (GBM) [14]. Genomic profiling by means of the array-comparative genomic hybridization (CGH) interrogation of 25 primary glioma cell lines has shown that the BAC clone encompassing MARK4 at 19q13.2, centromeric to the critical loss of heterozygosity (LOH) area [15], is included in a "gain" region in a few of these cell lines, and confirmed MARK4 duplication in the MI-4 glioblastoma cell line [16]. Array-CGH studies have also shown that aneuploidy affects many chromosomes in addition to the well-known chromosomes 7 and 10, which is in line with previous evidence of the complex genetic identity of human gliomas and increasing chromosomal instability during progression [17,18].

Ploidies ranging from near-diploid/aneuploid to near-triploid or near-tetraploid nuclear DNA have been reported in gliomas [17,19,20]. Tetraploidy, resulting from a failure in cytokinesis or in the G1/S checkpoint [21,22] has been described as a major route to the centrosome amplification contributing to aneuploidy and cancer development [23]. The MARK4L protein is highly expressed in cancers other than gliomas, including hepatocarcinoma [9] and leukemia cell lines (personal observations). In addition to its restricted expression by human neural progenitors in the CNS [10], this suggests that the L isoform plays a preferential role in cycling cells, whereas it has been reported that the MARK4S isoform, which is scarcely expressed in gliomas [10] and mainly expressed in adult brain [9, 10], is up-regulated in the early stages of an ischemic event that increases the likelihood of neuronal death [11]. The two complementary datasets support the general view that MARK4 may be involved in cell cycle control.

We here provide proteomic data relating to the assignment of endogenous MARK4L protein to the migrating 90 kDa band in gliomas. Immunoblot experiments using centrosome, midbody and nucleoli fractions purified from glioma cell lines merge to the immunofluorescence localization of MARK4L antibody, thus indicating multiplex gene entry into the cell cycle. A possible connection between MARK4L and centrosomal aberrations is suggested by MARK4L co-staining with the aberrant centrosome configurations observed in glioma cell lines.

2. Materials and methods

2.1. Cell cultures and tissue samples

The human primary glioma cell lines included G-91 (astrocytoma) (A), G-157 (oligoastrocytoma) (OA), MI-62 (anaplastic oligoastrocytoma) (AOA), G-1 (giant cell GBM) (GCGBM), and MI-60, MI-4 and MI-63 glioblastomas. All of the cell lines have been previously characterized by conventional cytogenetics [17] and 1 Mb resolution BAC array-CGH plus full coverage set for chromosome 19 [16]. The two oligoastrocytic cell lines MI-62 and G-157 included in this panel were not found to have loss of chromosome 19q. Cell lines were grown in RPMI supplemented with 5% fetal bovine serum at 37°C in humidified 5% CO_2. Normal human neural progenitor cells (NHNPs) (Lonza Walkersville, Inc., Verviers, Belgium) grown as neurospheres were kept in neural progenitor maintenance bulletkit according to the manufacturer's protocol. The human glioma samples were obtained immediately after surgery from patients who had received no previous chemotherapy or radiation treatment in accordance with a protocol approved by the Internal Review Board of the University of Milan's Neurosurgery Department, and the specimens were immediately processed for protein extraction. All of the cases were categorized on the basis of the WHO classification as A (#2), O (#1, #4, #6 and #7) and GBM (#3 and #5). Oligodendroglial tumors were tested for LOH by loss of D19S412, D10S112 and D19S219 markers. Only O (#7) showed loss of the 19q minimal deleted region.

2.2. Antibodies

The primary antibodies used for the immunofluorescence (IF) studies were the rabbit polyclonal MARK4L antibody, clone G86 (1:50, 1:100 dilution) (not commercial) [12] and monoclonal antibodies against γ-tubulin, clone GTU-88 (1:100, 1:200 dilution)

(Sigma, Saint Louis, MO), centrin (1:100, 1:150 dilution) (Sigma) and nucleolin, C23 D-6 (1:100 dilution) (Santa Cruz Biotechnology, Inc., Santa Cruz, CA). The secondary antibodies were goat anti-rabbit IgG conjugated to fluorescein isothiocyanate (FITC) (1:100 dilution) (Sigma) and goat anti-mouse IgG conjugated to FITC and tetramethylrhodamine isothiocianate (TRITC) (1:100 dilution) (Sigma). The antibodies were diluted in PBS with 0.1–0.5% Tween 20, 2% bovine serum albumin (BSA) and 1% goat serum (Sigma).

The primary antibodies used for immunoblotting were the rabbit polyclonal antibodies against MARK4L, clone G86 (1:1000, 1:2000 dilution) [12], and β-actin (1:1000, 1:2000 dilution) (Cell Signaling Technology, Inc., Beverly, MA), and the mouse monoclonal antibodies against γ-tubulin, clone GTU-88 (1:100, 1:200 dilution) (Sigma), nucleolin, clone C23 D-6 (1:100 dilution) (Santa Cruz Biotechnology, Inc.) and β-tubulin, clone Tub 2.1 (1:1000 dilution) (Sigma). The secondary antibodies, conjugated with horseradish peroxidase (HRP), were goat anti-rabbit IgG (1:10,000 dilution) and goat anti-mouse IgG-2b (1:10,000 dilution), both from Santa Cruz Biotechnology, Inc. The antibodies were diluted in TBS-T (1× TBS, 0.01% Tween 20).

2.3. Immunofluorescence and microscopy

For the better visualization of centrosomes, cells grown on glass chamber slides were washed in microtubule-stabilizing buffer (0.1% Triton X-100, 80 mM PIPES, pH 6.9, 5 mM EGTA, 1 mM MgCl) as described [8], fixed with 2% paraformaldehyde in PBS for 30 min on ice, and permeabilized in 0.2% Triton X-100 for 2 min. Different cells were washed in PBS, fixed with methanol for 10 min at -20°C or 2% paraformaldehyde, and permeabilized with 0.1% Triton X-100 for 10 min. The fixed cells were blocked with 5% BSA in PBS for 10 min before incubation with the primary antibodies. MARK4L, γ-tubulin and centrin were incubated overnight at 4°C; nucleolin was incubated for one hour at room temperature (RT).

In dual-labelled immunoreactions, after three washes in PBS, the secondary antibodies anti-rabbit IgG-FITC and/or anti-mouse IgG-TRITC were incubated for one hour at RT in a humidified chamber. The slides were then mounted with 4′,6′-diamidino-2-phenylindole (DAPI) in antifade (Vector Labs, Burlingame, CA) and examined using an Olympus IX51 inverted fluorescence microscope, equipped with an Olympus DP71 super high-resolution colour digital camera and U-MNIBA2 excitation 460/490 (FITC), U-MWIG3 excitation 530/550 (TRITC) and U-MNU2 (DAPI) filters. The images were acquired and processed using the F-View II-Bund-cell F software (Olympus).

2.4. Silver stain for nucleoli

Cells previously showing MARK4L immunoreactivity in subnuclear domains under baseline IF conditions were washed in PBS and covered with 60 µl of a staining solution consisting of 50% silver nitrate and 2% gelatine in 1% aqueous formic acid in accordance to Korek et al. [24], and kept at 37°C for 10 min. The slides were then washed several times in distilled water and mounted in Vectashield Mounting Medium (Vector Labs, Burlingame, CA).

2.5. Analysis of aberrant centrosomes

Centrosome anomalies were analysed by means of fluorescence microscopy using anti-MARK4L [12] and γ-tubulin antibodies [25]. On the basis of findings in non-malignant control cells, the interphase and metaphase centrosomes were considered abnormal if there were more than two copies per cell and/or if they were organised in large clusters [26].

2.6. Centrosome isolation

Centrosomes were isolated from the glioblastoma cell lines as described [27] with minor modifications. The cells (5×10^7) were incubated with 1 µg/ml of cytochalasin B (Sigma-Aldrich) and 1 µg/ml of nocodazole (Sigma-Aldrich) for one hour, and the pellet was rinsed once in 1× TBS and 0.1× TBS/8% sucrose. They were then resuspended in 2 ml of 0.1× TBS/8% sucrose, followed by the addition of 8 ml of lysis buffer (1 mM HEPES, pH 7.2, 0.5% Nonidet P-40 (NP-40), 0.5 mM $MgCl_2$, 0.1% β-mercaptoethanol, protease (Roche Diagnostics, Manheim, Germany) and phosphatase inhibitor cocktails (Pierce Biotechnology, Rockford, IL)). The suspension was gently pipetted several times and spun at 2500g for 10 min; the supernatant was filtered through a 40–50 µm nylon membrane, supplemented with HEPES buffer to a final concentration of 10 mM and DNase I (2 U/ml) (Invitrogen, Carlsbad, CA), and incubated on ice for 30 min. The mixture was gently underlaid with 1 ml of a 60% sucrose solution (10 mM PIPES, pH 7.2, 0.1% Triton

X-100 and 0.1% β-mercaptoethanol containing 60% sucrose w/v) and spun at 10,000g for 30 min to sediment centrosomes. The upper 8 ml was removed and the remaining part, containing the concentrated centrosomes, was vortexed and loaded onto a discontinuous sucrose gradient consisting of a 70%, 50% and 40% w/v solution from the bottom (500 µl 70% sucrose, 300 µl 50% sucrose and 300 µl 40% sucrose) and spun at 120,000g for 1 h. Fractions of 200 µl were collected from the bottom, immediately frozen in liquid nitrogen and stored at -80°C.

2.7. Midbody isolation

Midbody isolation was based on a described method [28]. Cells from the glioblastoma cell lines (5×10^7) were incubated with 400 ng/ml of nocodazole and, after 12 hours, were released from mitotic arrest in nocodazole-free medium for 25 min. The pellet was resuspended in a hypotonic swelling solution (1 M hexylene glycol, 20 µM $MgCl_2$, 2 mM PIPES, pH 7.2) containing taxol (10 µM) at RT and immediately centrifuged at 200g for 3 min, before being suspended in 50 ml of lysis solution (1 M hexylene glycol, 1 mM EGTA, 1% NP-40, 2 mM PIPES, pH 7.2) containing protease and phosphatase inhibitor cocktails and taxol (10 µM) at 37°C. The lysate was then vigorously vortexed for 1 min to ensure complete midbody release and chilled on ice. After the addition of cold 0.3 ml of 1 M hexylene glycol, 50 mM 2-morpholinoethanesulfonic acid (MES), pH 6.3, the lysate was centrifuged at 250g for 20 min to remove large debris and the supernatant was layered over a cushion of 40% glycerol (w/v) in 50 mM MES buffer and spun at 2800g for 20 min to pellet the midbodies. The glycerol step was repeated and, after a final wash with MES buffer, the midbodies were stored at -80°C.

2.8. Nucleoli isolation

Nucleoli were prepared using a variation of a described method [29]. Cells from the glioblastoma cell lines (7×10^7) were washed with pre-warmed fresh medium one hour before nucleolar isolation, and then three times with pre-warmed PBS before trypsinization. The pellet was washed twice in PBS, resuspended in cold buffer A (10 mM HEPES, pH 7.9, 10 mM KCl, 1.5 mM $MgCl_2$, 0.5 mM dithiothreitol (DTT) and protease inhibitors), and incubated on ice for 5 min. The swollen cells were controlled under a phase contrast microscope (Olympus IX51) and the suspension was then transferred to a pre-cooled 7 ml dounce tissue homogenizer (Wheaton Scientific, Millville, NJ), homogenized several times until $\geqslant$90% of the cells had burst and spun at 1000 rpm for 5 min at 4°C. The pellet was resuspended with 3 ml of S1 solution (0.25 M sucrose, 10 mM $MgCl_2$ and protease inhibitors) by pipetting up and down, layered over 3 ml of S2 solution (0.35 M sucrose, 0.5 mM $MgCl_2$, protease inhibitors) and spun at 2500 rpm for 5 min at 4°C. The resulting pellet was resuspended with 3 ml of S2 and sonicated for six 10-s bursts (with 10-s intervals between each burst) using a Misonix XL 2000 sonicator (Misonix, Inc., Farmingdale, NJ), after which the sonicated nuclei were checked under a phase contrast microscope. The suspension was layered over 3 ml of S3 solution (0.88 M sucrose, 0.5 mM $MgCl_2$, protease inhibitors) and spun at 3500 rpm for 10 min at 4°C. The pellet containing the nucleoli was then resuspended in 0.5 ml of S2 and stored at -80°C.

2.9. Preparation of cell extracts from cell lines and tissue samples

The cells were harvested, washed in PBS, counted and incubated in 1 ml lysis buffer/10,000,000 cells; 50 mg of tissue sample were homogenized using a tissue homogenizer (Wheaton Scientific) in 1 ml of lysis buffer (150 mM NaCl, 50 mM Tris, pH 7.5, 1% NP-40, 0.25% deoxycholic acid, protease inhibitors, 1 mM sodium orthovanadate, 1 mM phenylmethanesulphonylfluoride). The suspensions were placed on ice for 30 min with occasional inversion to ensure complete lysis. All of the subsequent passages were done at 4°C. The lysates were pelleted for 25 min at 16,000g and the supernatant (whole cell lysate) was incubated with 1:100 Protein G Sepharose 4 Fast Flow (GE Healthcare, Waukesha, WI) for 30 min with occasional inversion, in order to eliminate any unspecific binding with the secondary antibody; the lysate was pelleted for 25 min at 16,000g and the clarified supernatant was stored at -20°C. Protein concentration was determined using the BCA Protein Assay Kit (Pierce), according to the manufacturer's protocol.

2.10. Immunoprecipitation

Whole lysates from the glioma cell lines and tissue samples were incubated overnight at 4°C with 1:50 anti-MARK4L antibody, in agitation, and then with 50–100 µl of Protein G Sepharose 4 Fast Flow for 3 h at 4°C. Centrifugation at 16,000g for 3 min at 4°C

precipitated the sepharose-protein G-anti-MARK4L antibody-MARK4L complex, which was then washed three times in lysis buffer. After the last centrifugation, the pellet was resuspended in reducing SDS loading buffer (Cell Signaling Technology, Inc.) and denatured at 95°C for 5 min. After centrifugation at 16,000g for 3 min at 4°C, the protein-containing supernatant was loaded onto a polyacrylamide gel.

2.11. SDS-PAGE and immunoblotting

The lysates were prepared by adding reducing SDS loading buffer (SB) to equal amounts of the extracted proteins and denatured at 95°C for 3 min. The centrosomes of each fraction were first sedimented by adding 1 ml of 10 mM PIPES, pH 7.2, and centrifuging at 20,000g for 15 min at 4°C. The supernatants were removed and the centrosomes resuspended in SB. The nucleoli were pelleted at 20,000g for 20 min at 4°C and resuspended in SB.

The proteins were separated by means of 4% (stacking) and 10% (resolving) SDS polyacrylamide gel electrophoresis and subsequently stained with Simplyblue Safestain (Invitrogen) or transferred by electroblotting to a polyvinylidene fluoride (PVDF) membrane (Roche) for immunoblot analyses. Mini-PROTEAN 3 Cell and Trans-Blot Semi-dry Electrophoretic Transfer Cell (both Bio-Rad, Hercules, CA) were respectively used for electrophoresis and electroblotting as instructed by the manufacturer. The molecular weight standards were Benchmark Protein Ladder (Invitrogen) for Coomassie-stained gels and Biotinylated Protein Ladder (Cell Signaling) for the immunoblots. Non-specific binding was blocked by incubating the membranes in 5% BSA, 1× TBS, 0.1% Tween 20 for two hours at RT, in agitation. The membranes were then incubated overnight with primary antibodies, in agitation, washed three times (5–10 min each) in 1× TBS, 0.01% Tween 20 (TBS-T) and then incubated with secondary antibodies at RT for two hours, in agitation. After three washes in TBS-T, the bound antibodies were detected by covering the membrane with Supersignal West Pico Chemiluminescent Substrate (Pierce) for 5 min, exposing an Amersham Hyperfilm MP (GE Healthcare) to the membrane, and developing the film by Dental X-Ray Developer and Dental X-Ray Fixer (KODAK). The images were acquired from gels and films using a Chemidoc XRS CCD camera and Quantity One software (both Bio-Rad).

2.12. Mass spectrometry

The Coomassie blue-stained protein bands were excised from SDS gel and *in vitro* digested by trypsin to yield a mixture of peptides generated on the basis of the presence of arginine and lysine residues in the original protein chain. The peptide mixture was then analysed by MALDI-TOF mass spectrometry (MS), which gives the accurate molecular weights of some or most of the peptides. The MALDI-MS analyses were carried out using a Voyager DE PRO reflectron (Applied Biosystem, Firmingham, MA). Typically, 1 µl of analyte solution was loaded onto the MALDI sample plate and mixed with the same volume of a 10 mg/ml solution of α-cyano-4-hydroxy cinnamic acid or synapinic acid as matrix. The spectra were acquired and processed using the software provided by the manufacturer. The peptide masses of each digested protein were used to interrogate protein databases using the Peptide Mass Fingerprinting (PMF) Mascot from Matrix Science.

Using the Expasy website (http://www.expasy.org/tools/peptide-mass.html), we made a virtual tryptic digestion of the known MARK4L sequence to obtain a list of peptide masses. The specific requirements were: (i) the selected enzyme was trypsin; (ii) the maximum number of miss cleavages was two; (iii) all cysteines were treated with iodoacetamide to form carbamidomethyl-cysteine, a peptide with a mass of $>$500 Dalton; and (iv) monoisotopic masses of the occurring amino acid residues with peptide masses of $(M+H)^+$. In the total spectrum of the peptide mixture and the zoomed portions, we looked for the specific peaks belonging to the obtained list.

3. Results

3.1. Western blot and immunoprecipitation specificity of MARK4L antibody in gliomas and NHNPs

The immunoreactivity of the specific anti-MARK4L antibody (clone G86, not commercial) against the *in vitro* synthesized human MARK4L isoform and protein extracts from normal mouse brain migrating on SDS gel at 90 kDa has been reported [12]. We here tested this antibody against the endogenous human MARK4L protein in glioma cell lines, fresh glial tumours and NHNPs extracts using Western blot analysis. As shown in Fig. 1A and B, all of the cell lines, NHNPs and tissue extracts showed a band at 90 kDa

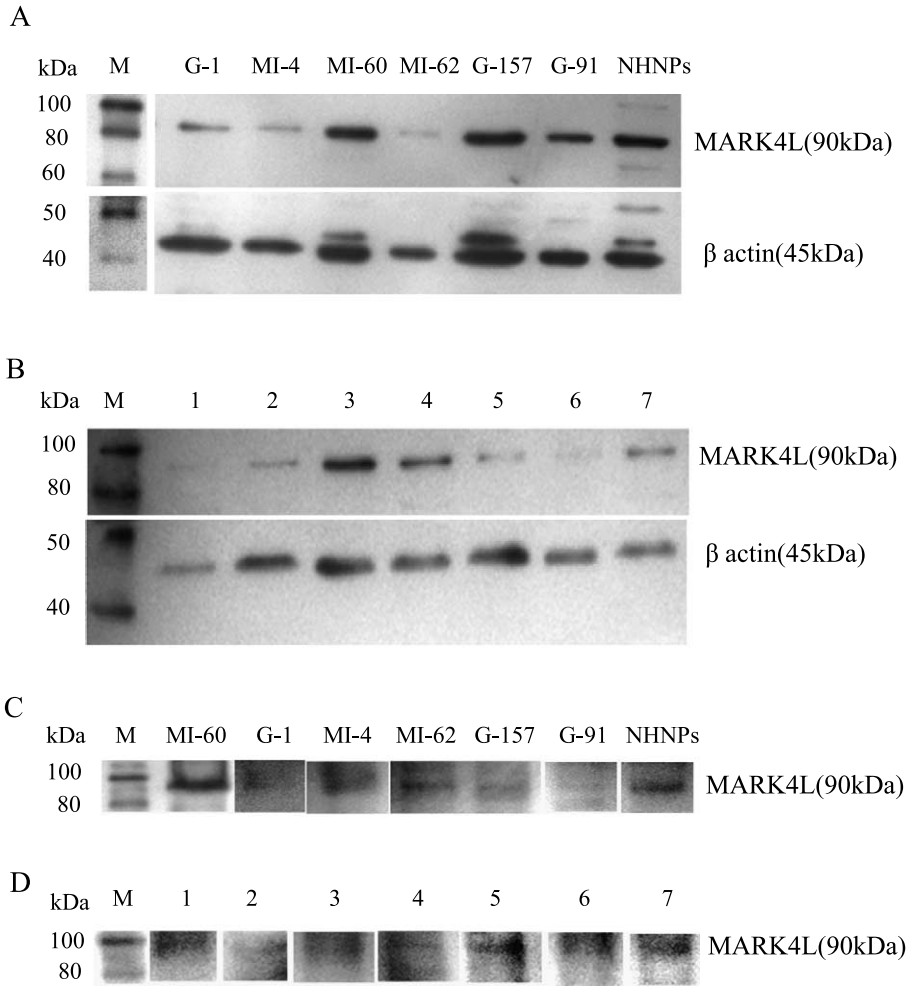

Fig. 1. (A) Immunoblots with anti-MARK4L antibody on a panel of whole cell lysates from glioma cell lines G-1 (GCGBM), MI-4, MI-60 (GBM), MI-62 (AOA), G-157 (OA) and G-91 (A), and normal human neural progenitor cells (NHNPs). (B) Immunoblots with anti-MARK4L antibody on cell lysates from fresh gliomas 2 (A), 1, 4, 6, 7 (O), 3 and 5 (GBM). The samples were normalized using β-actin. (C and D) Immunoblots with anti-MARK4L antibody on whole cell lysates from the glioma cell lines and fresh gliomas, immunoprecipitated with anti-MARK4L antibody. M: molecular weight ladders (kDa).

immunoreacting with MARK4L antibody in addition to a few other faint bands. The apparent variability in MARK4L expression by gliomas of different subtype and grade is currently under study on a much wider number of snap frozen tumour tissues from well-documented patients including adequate follow-up data.

We also used immunoprecipitation assays on lysates of the same cell lines, NHNPs and fresh tumours to test the antibody. The blot labelled a band at 90 kDa, showing the ability of the antibody to immunoprecipitate MARK4L (Fig. 1C and D). The protein was not detected by the pre-immune serum (Suppl. Fig. 1: http://www.qub.ac.uk/isco/JCO).

3.2. Assignment of the endogenous MARK4L protein within the ∼90 kDa band by mass spectrometry

MARK4L is ubiquitously expressed [9] thus preventing the use of a negative control devoid of the antigen of interest. Thus, in order to minimize unrecognized cross-reactivity, we validated the specificity of the immunocytochemical experiments by checking the identity of the recognized protein by means of mass spectrometry. Figure 2A shows the Coomassie-stained gel of MI-60 cell line taken as a representative example.

Bands migrating around 90 kDa from whole cell lysate and the lysate immunoprecipitated with anti-

A

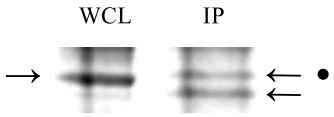

B

MW (Da)	PEPTIDES (aa)
617,04	402-407
777,10	30-36
901,47*	290-297
1179,50	298-306
1194,55*	26-36
1201,54	14-25
1236,52*	78-88
1265,53	299-308
1275,60*	437-448
1320,47	679-689
1365,54*	411-421
1411,55	334-345
1475,65	732-745
1513,66*	357-369
1634,76	726-740

MW (Da)	PEPTIDES (aa)
1678,44	26-41
1707,68	78-92
1717,60	275-288
1836,30	402-418
1937,82	493-509
1993,03	26-43
2002,83	89-105
2016,71	539-558
2085,80	438-456
2106,71	387-407
2113,87	437-455
2286,82	350-369
2304,15	93-111
2385,74	357-377 or 89-108

C

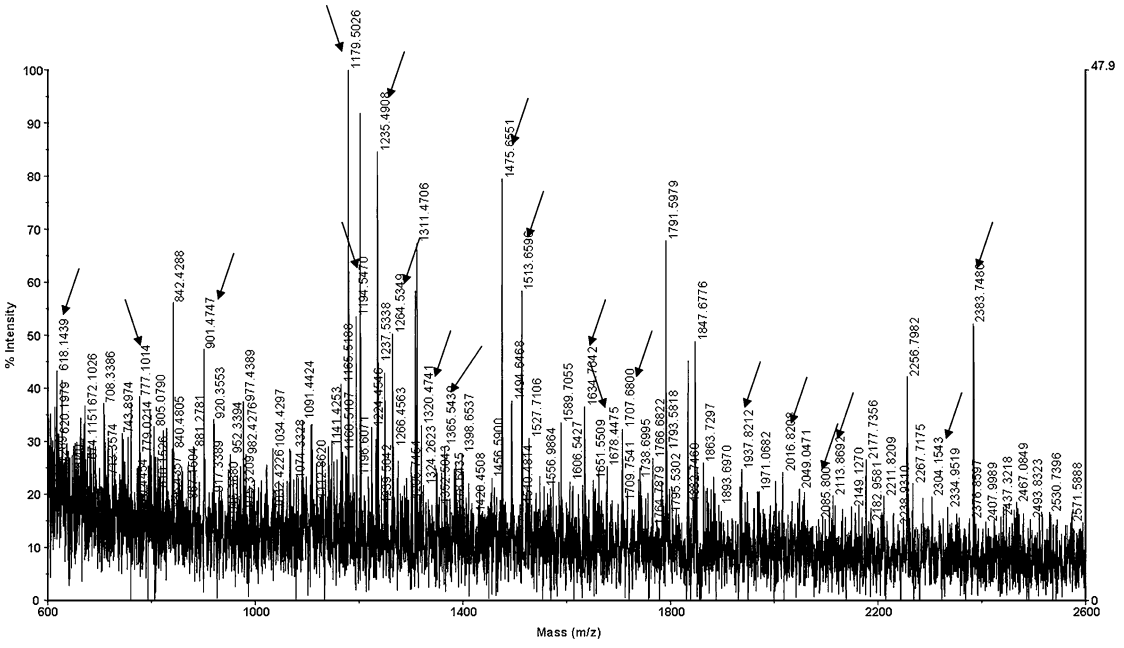

Fig. 2. (A) Coomassie-stained gel of MI-60 whole cell lysate (WCL) and MI-60 lysate immunoprecipitated with anti-MARK4L antibody (IP). The bands migrating around 90 kDa (arrowed) were excised and processed by mass spectrometry. (B) Set of 29 mass signals found within the MARK4L IP protein band (● in Fig. 2A) assigned to the corresponding peptides within the MARK4L sequence. The asterisks indicate the mass values matching those within the MARK4L WCL band. (C) MALDI-mass spectrum (ranging from 600 to 2600 Dalton) of the digested peptides from the 90 kDa IP band (● in Fig. 2A). Of the 29 signals assigned to MARK4L, only 20 (arrowed) are visible because of the compactness of the mass spectrum; the other nine are visible in zoomed portions of the spectrum (not shown).

MARK4L (Fig. 2A, arrowed) were excised and gel-digested as described and the peptide mixture was processed by MALDI-TOF. The *in silico* search in public protein databases indicated a low probability score for the MARK4L protein and so we made a virtual tryptic digestion of MARK4L protein sequence and then a manual search to find molecular weight (MW) signals belonging to MARK4L in the spectrum. A number of peaks were assigned to regions of MARK4L and, in particular, we found 29 MW values of peptides (Fig. 2B) coming from the MARK4L sequence in the immunoprecipitated protein band (indicated by a dot in Fig. 2A) that led to 33% coverage of the primary structure. Although some sequence portions could not be mapped, the coverage obtained is more than adequate for protein identification. Conversely, the other immunoprecipitated 90 kDa band did not contain any MARK4L peptides (not shown). The band excised from the whole cell lysate showed the mass values indicated by the asterisks in Fig. 2B. The MALDI mass spectrum in Fig. 2C shows the mass signals assigned to the corresponding peptides of MARK4L after virtual tryptic identification. These findings confirmed that MARK4L protein is present within the ∼90 kDa band.

3.3. *The endogenous MARK4L protein localizes to normal and aberrant interphase/mitotic centrosomes, midbodies and nucleoli in glioma cell lines*

On the basis of previous evidence of an association between exogenous MARK4 and interphase centrosomes [8], we used IF to determine the subcellular distribution of the endogenous protein. Under microtubule-stabilizing conditions, we observed a MARK4L-specific signal in the nuclear/perinuclear region of the interphase cells, giving rise to variously sized single and multiple fluorescent dots (Suppl. Fig. 2: http://www.qub.ac.uk/isco/JCO). Co-labelling with MARK4L and γ-tubulin antibodies against the main centrosomal protein confirmed that MARK4L has a centrosomal localization and revealed two kinds of abnormal perinuclear distribution in the investigated glioma cell lines: a clustered (Fig. 3A, top) and a random one (Fig. 3A, bottom). The latter is peculiar to glioblastoma cell lines, whereas the former is shared by low and high grade gliomas and is most frequently observed. Dual-colour IF with γ-tubulin and centrin antibodies showed that the abnormal centrosomes were structurally conserved, which confirmed the co-presence of these key centrosomal components (Suppl. Fig. 4: http://www.qub.ac.uk/isco/JCO).

Under baseline IF conditions, MARK4L labelled large subnuclear domains indicating the nucleolar localization of the endogenous protein. The targeted structures were confirmed as nucleoli by means of the silver colloid method, which revealed a number of silver grains co-labelled with anti-MARK4L (Fig. 3B, left panel), and dual IF staining with anti-nucleolin antibody (Fig. 3B, right panel). Our results showed differences in nucleolar frequency and size depending on the subtype of glioma cell lines and according to previously data on brain tumours [30].

Information concerning MARK4L localization throughout cell division was acquired by analysing the same glioblastoma cell line at different stages of mitosis using MARK4L and γ-tubulin antibodies. During prometaphase and metaphase, MARK4L was concentrated at the spindle poles and associated with microtubules growing between the two asters; at anaphase, it was detected in the midzone and, at late anaphase, it was repositioned outside the nucleus. The mitotic centrosome appears as an aggregate of fluorescent dots co-stained with MARK4L antibody (Fig. 3C). In addition, MARK4L gave a bright fluorescent signal in the centre of the midbody at the contact point between the two daughter cells during cytokinesis (Fig. 3D). No specific fluorescence was seen using pre-immune serum or the secondary antibodies without primary antibodies (data not shown).

3.4. *MARK4L antibody immunoreacts with subcellular fractions of centrosomes, midbodies and nucleoli in glioma cell lines*

Centrosomes, midbodies and nucleoli were isolated from the MI-4, MI-60 and MI-63 GBM cell lines by means of biochemical fractionation and analysed for the presence of MARK4L by means of Western blotting. Centrosome-enriched fractions obtained on sucrose gradients showed a parallel distribution of MARK4L and γ-tubulin proteins, with the strongest signals of both proteins being observed in fractions 2 and 3, corresponding to 60–70% w/v sucrose, where centrosomes are known to sediment [27] (Fig. 4A). Moreover, as centrosomes were isolated after treatment with nocodazole, which is known to depolymerise microtubules, the association of MARK4L with centrosomes appears to be microtubule-independent. Immunoblotting analysis of the midbody and nucleoli fractions also detected the endogenous pro-

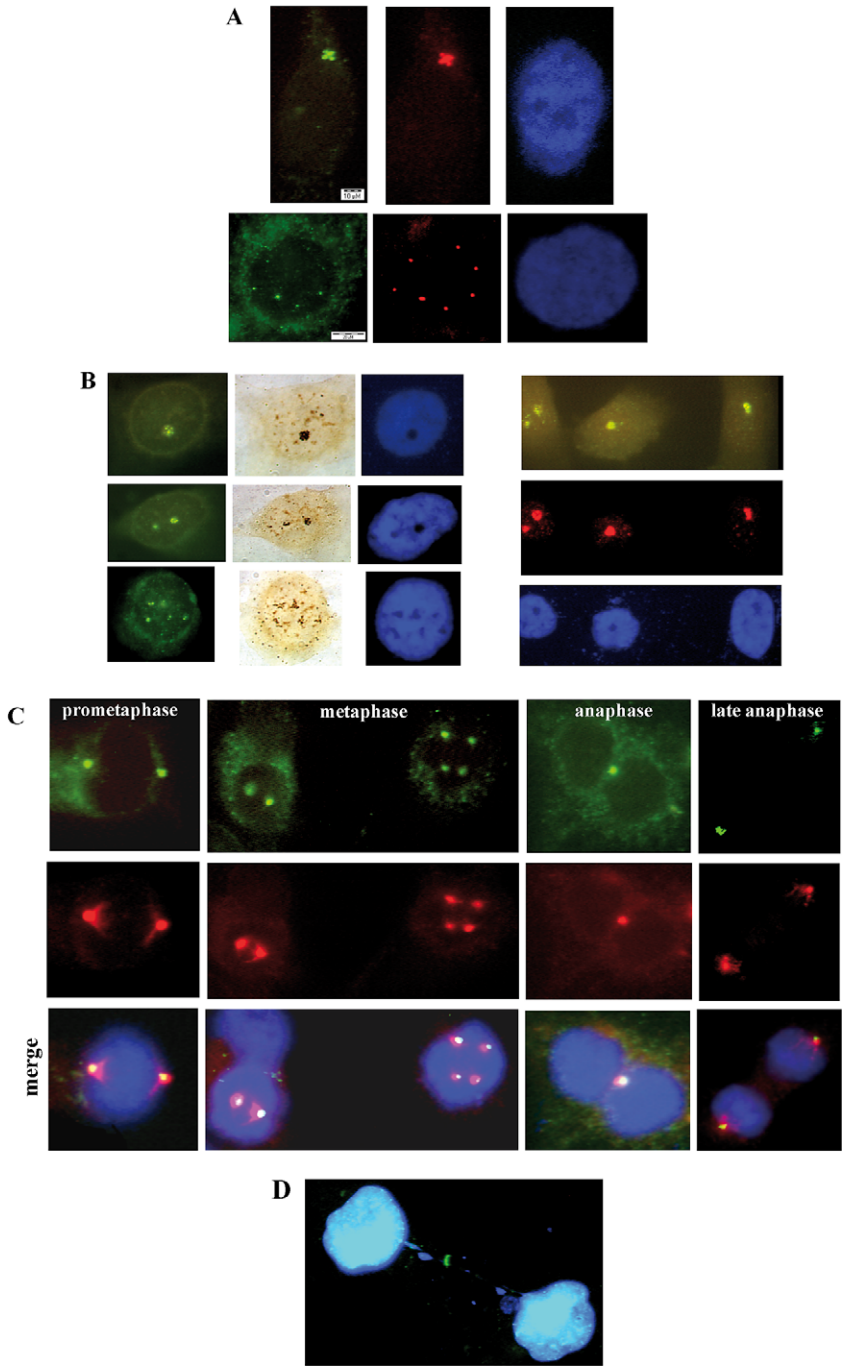

Fig. 3. Subcellular localization of MARK4L in glioma cell lines as revealed by IF. Magnification 63× or 100×. Scale bars = 10 μm (A, top), 20 μm (A, bottom). The nuclei are counterstained with DAPI. (A) Double MARK4L (green)- and γ-tubulin (red)-immunostained photomicrographs of MI-60 interphase cells showing the two main configurations of amplified centrosomes: a large clustered signal (top) and multiple random signals (bottom). (B) Anti-MARK4L antibody (green) and silver-colloid method showing nucleolar localization of MARK4L signals in G-91, MI-60 and MI-4 cells (left panel, top to bottom). Double-immunostaining of MARK4L (green) and nucleolin (red) showing co-localization to the nucleoli in MI-60 cells (right panel). (C) Cells from the MI-60 cell line representative of all mitotic phases following dual IF labelling with MARK4L (green) and γ-tubulin (red). (D) Localization of MARK4L (green) to the midbody formed during cytokinesis in MI-60 cells.

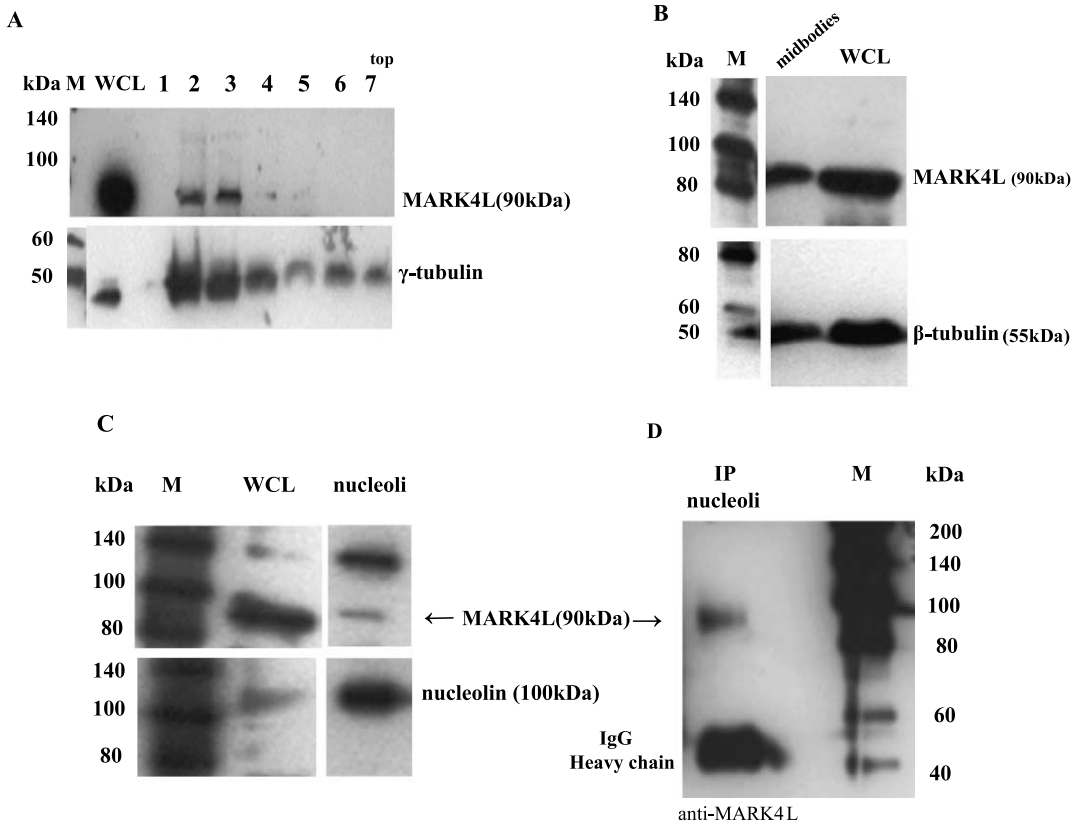

Fig. 4. (A) Immunoblot analysis of whole cell lysate (WCL) and centrosome fractions (1–7) from the MI-4 cell line. Upper panel: immunostaining with anti-MARK4L antibody; lower panel: immunostaining with anti-γ-tubulin antibody. (B) Immunoblot analysis of midbodies and whole cell lysates from the MI-60 cell line. Upper panel: immunostaining with anti-MARK4L antibody; lower panel: immunostaining with anti-β-tubulin antibody. (C) Immunoblot analysis of whole cell lysate and nucleoli from the MI-60 cell line. Upper panel: immunostaining with anti-MARK4L antibody; lower panel: immunostaining with anti-nucleolin antibody. (D) Nucleoli fraction immunoprecipitated and immunostained with anti-MARK4L antibody. M: molecular weight ladders (kDa).

tein in the assayed subcellular components; the integrity of the midbody and nucleoli fractions was respectively confirmed by β-tubulin and nucleolin markers (Fig. 4B and C). IP with MARK4L antibody of nucleoli fraction only showed the 90 kDa MARK4L band (Fig. 4D), thus attesting that the 130 kDa band visible in the Western blot (Fig. 4C) was due to crossreactivity. The absence of γ-tubulin signal in the nucleoli fraction attested the fraction purity (Suppl. Fig. 3: http://www.qub.ac.uk/isco/JCO), confirming that MARK4L signal in nucleoli is not due to centrosome contamination.

3.5. *Morphological analysis of centrosome aberrations in glioma cell lines*

The co-immunolocalization of MARK4L and γ-tubulin antibodies showed the association of the kinase with the aberrant centrosomes in the investigated glioma cell lines. Detailed morphological analysis of the aberrant centrosomes by γ-tubulin antibody showed that the interphase centrosome cluster (Fig. 3A, top) always had the same morphology, as shown by the representative images obtained from different grade glioma lines (enlargement in Fig. 5A). An abnormal distribution of centrosomes at the nuclear poles was occasionally visible in the cell nuclei approaching mitosis (Fig. 5B). The aberrant metaphase centrosomes revealed mitotic spindles of very different sizes and shapes that were nonetheless able to nucleate microtubules (Fig. 5C).

4. Discussion

We performed this study as our and previously published data suggested that the L isoform of MARK4

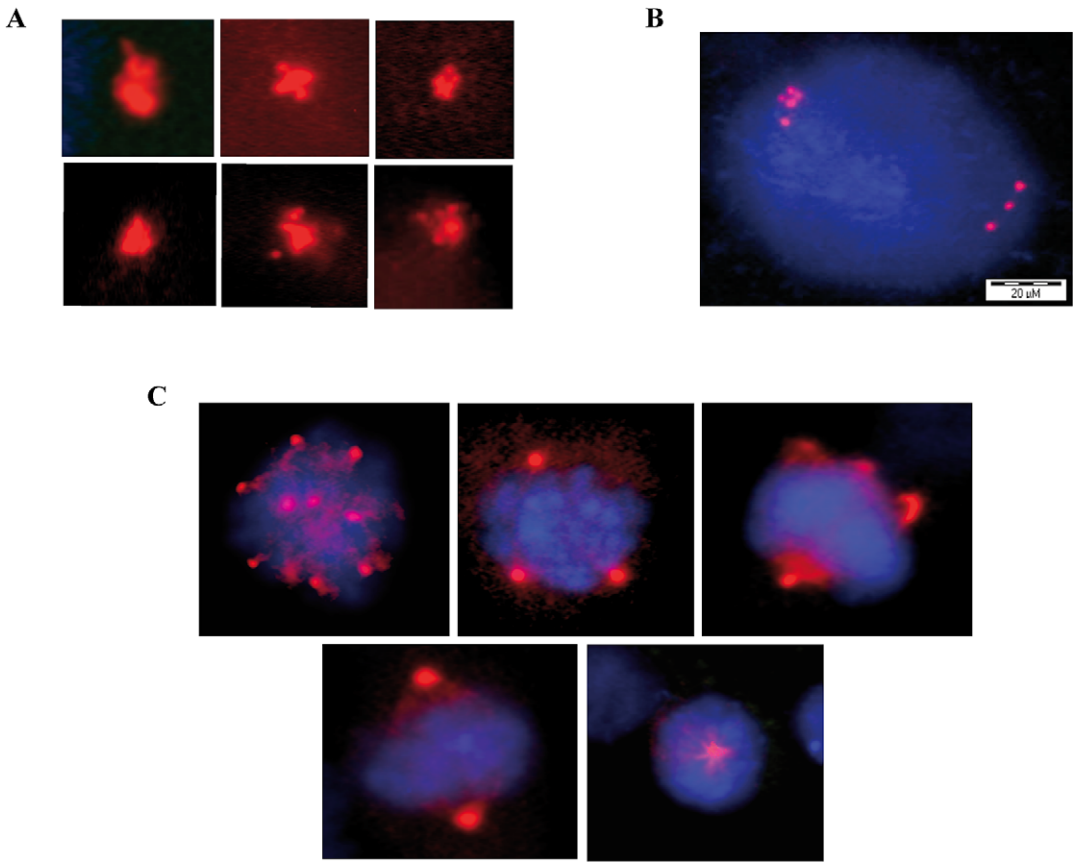

Fig. 5. Immunofluorescence with anti-γ-tubulin antibody (red) showing morphological features of aberrant centrosomes in the glioma cell lines. Magnification 63× or 100×. Scale bars = 20 µm (A, B, C). DNA was counterstained with DAPI (blue). (A) Centrosomes with a clustered distribution and similar morphology in the different cell types. (B) Abnormal distribution of centrosomes at nuclear poles in a cell entering mitosis. (C) Abnormal mitotic spindles: multipolar, tripolar, bipolar with one centrosome at one pole and three at the other, pseudobipolar with larger centrosomes than those of a normal bipolar spindle, monopolar.

plays a role in proliferating cells [9,10], and it has been postulated that exogenous MARK4 might play a more general role in regulating centrosomal activities and microtubule organization [8]. Lack of knowledge on the subcellular localization of the endogenous MARK4L protein prompted us to address this topic by analysing selected glioma cell lines with a specific anti-MARK4L antibody, previously used on normal mouse brain [12]. We validated MARK4L specificity against human cell lines and fresh gliomas of different malignancy in parallel with undifferentiated human neural progenitors (NHNPs).

The *in silico* search in protein databases showed low score of the MARK4L protein, which may be consistent with an undetectably low level of expressed protein [31] that allows other more abundant and co-migrating 90 kDa proteins to mask the specific MARK4L signals. However, the manual search by virtual tryptic digestion identified peptide sequences belonging to MARK4L. Comparison of the MARK4L mass signals revealed by the two approaches allowed the protein kinase to be unambiguously assigned within the ∼90 kDa band.

Our findings show that endogenous MARK4L has two distinct locations in interphase glioma cell lines, depending on the fixation method (which is known to produce somewhat different staining patterns) [32,33]. We found the location outside the nucleus consistent with the centrosome, whereas the sub-nuclear dots are compatible with a nucleolar localization. During mitosis, MARK4L is associated with the centrosome at all stages of division, and appears in the centre of the midbody in cytokinesis. Its immunocytochemical localization fairly matches the biochemical analysis of isolated centrosomes, midbodies and nucleoli, thus supporting the presence of the 90 kDa MARK4L protein in the

same sub-cellular fractions. On one hand these findings are in keeping with previous evidence of the exogenous association of MARK4 with interphase centrosomes [8], on the other hand immunofluorescence highlighted new and distinctive sub-cellular locations of MARK4L by showing its association with mitotic centrosome, midbody and nucleolus activity during the cell cycle. The centrosome association of MARK4L was not abolished by the nocodazole-induced depolimerization of microtubules, thus suggesting that the kinase is a core component of centrosomes.

Various other proteins with a regulatory function during cell cycle progression have also been shown to have a centrosome localization in inter- and metaphase, and have been found to accumulate at the midbody in cytokinesis. Such multiple localizations are exemplified by the so-called "chromosome passengers", such as Aurora [34], Plks [35] and Nek2 [31] mitotic kinases, and phosphoproteins such as CEP170 [34] and CEP55 [36]. Interestingly, the dynamic localization of some of these proteins is regulated by multiple phosphorylation/dephosphorylation events [35]. It is known that, like other members of the MARK family, MARK4 plays an important role in regulating the transition between stable and dynamic microtubules through phosphorylation by LKB1 [4] and, interestingly, it has recently been proposed as a potential candidate in the regulation of the novel doublecortin-like kinase (DCLK) MAP during neurogenesis because its expression is restricted to neural progenitors in CNS [37].

Besides acting as microtubule-organizing centres, centrosomes also play an active role in cell cycle progression and in the prevention of premature cytokinesis thus ensuring genome stability [38]. The final stage of cytokinesis occurs at the midbody, a transient structure which, in addition to proteins indispensable for the completion of cytoplasmic division, also contains a large range of functional proteins including asymmetric cell division and chromosome segregation proteins [39].

Some clues to the physiological role of MARK4 (PAR-1) [40] come from a study of orthologue "partitioning defective" (PAR) proteins [41] showing that asymmetrical PAR-1 proteins control the partitioning of *C. Elegans* zygote and embryonic axis formation in *Drosophila* by influencing cytoskeleton dynamics [42]. The localization of MARK4L in nucleoli during interphase is an intriguing finding. The reported link between the nucleolus and Alzheimer's disease (AD), which suggests a reduction in ribosomal gene activity in AD patients [43], the immunodetection of a nucleolar tau-MAP protein in human brain cells [32], and the specific role of the MARK family in phosphorylating the microtubule-associated protein tau in Alzheimer neurofibrillary degeneration all provide evidence of a possible relationship between MARK4L and the nucleolus.

The co-staining of aberrant centrosomes by MARK4L and γ-tubulin antibodies suggests a possible connection between the kinase and centrosomal aberrations in the glioma cell lines. Among isolated studies of centrosome abnormalities in glioma [26,44], a recent study of astrocytic gliomas and glioblastoma cell lines found supernumerary centrosomes associated with an increased expression of γ-tubulin, a key structural protein of centrosomes [25]. Despite their abnormal configuration, the centrosomes analysed in our study conserved their γ-tubulin and centrin centrosomal components, and it is worth noting that the prevalent clustered interphase centrosome configuration had the same morphology in the different cell lines as if the centrosomal aggregates were forced to adopt a fixed shape (Fig. 5A). The centrosome-like structures revealed by immunofluorescence can nucleate microtubules and contribute to the assembly of very different mitotic spindles, which indicate that extra centrosomes do not always lead to multipolar spindles. The coalescence of centrosomes to establish a bipolar division has been well documented in both cancer [45] and non-cancer cells [46,47], and it has recently been proposed that the suppression of multipolarity may be an intriguing mechanism by which cancer cells escape apoptosis [48].

Our and other published data reinforce the view that giant "compound" centrosomes capable of coalescing into a functional bipolar spindle favour mitotic stability and neoplastic growth. Our results are in line with the view that MARK4 is a multifunctional protein acting throughout the cell cycle. The direct or indirect involvement of MARK4L in regulating different subcellular compartments throughout the cell cycle remains to be acquired through studies of MARK4L interactors, while MARK4L siRNA-mediated depletion and/or overexpression should assess whether and how MARK4L contributes to the pathomechanisms of human glioma.

Acknowledgements

The authors would like to thank Dr. Angela Pontillo (PRIMM, Milan, Italy) for her expert assistance

in interpreting the mass spectrometry data. This study was supported by a grant from the *Associazione Italiana per la Ricerca sul Cancro* (Grant No. 4217 to L.L. for 2008). C.N. is a PhD student of Experimental Neuropathology at the University of Milan.

References

[1] G. Drewes, B. Trinczek, S. Illenberger, J. Biernat, G. Schmitt-Ulms, H.E. Meyer, E. Mandelkow and E. Mandelkow, Microtubule-associated protein/microtubule affinity-regulating kinase (p110^{mark}). A novel protein kinase that regulates tau-microtubule interactions and dynamic instability by phosphorylation at the Alzheimer-specific site serine 262, *Journal of Biological Chemistry* **270** (1995), 7679–2688.

[2] A. Ebneth, G. Drewes, E.M. Mandelkow and E. Mandelkow, Phosphorylation of MAP2c and MAP4 by MARK kinases leads to the destabilization of microtubules in cells, *Cell Motility and the Cytoskeleton* **44** (1999), 209–224.

[3] T. Timm, X.Y. Li, J. Biernat, J. Jiao, E. Mandelkow, J. Vandekerckhove and E.M. Mandelkow, MARKK, a Ste20-like kinase, activates the polarity-inducing kinase MARK/PAR-1, *EMBO Journal* **22** (2003), 5090–5101.

[4] J.M. Lizcano, O. Göransson, R. Toth, M. Deak, N.A. Morrice, J. Boudeau, S.A. Hawley, L. Udd, T.P. Mäkelä, D.G. Hardie and D.R. Alessi, LKB1 is a master kinase that activates 13 kinases of the AMPK subfamily, including MARK/PAR-1, *EMBO Journal* **23** (2004), 833–843.

[5] Y.M. Chen, Q.J. Wang, H.S. Hu, P.C. Yu, J. Zhu, G. Drewes, H. Piwnica-Worms and Z.G. Luo, Microtubule affinity-regulating kinase 2 functions downstream of the PAR-3/PAR-6/atypical PKC complex in regulating hippocampal neuronal polarity, *Proceedings of the National Academy of Science of the United States of America* **103** (2006), 8534–8539.

[6] O. Göransson, M. Deak, S. Wullschleger, N.A. Morrice, A.R. Prescott and D.R. Alessi, Regulation of the polarity kinases PAR-1/MARK by 14-3-3 interaction and phosphorylation, *Journal of Cell Science* **119** (2006), 4059–4070.

[7] D. Matenia, B. Griesshaber, X.Y. Li, A. Thiessen, C. Johne, J. Jiao, E. Mandelkow and E.M. Mandelkow, PAK5 kinase is an inhibitor of MARK/Par-1, which leads to stable microtubules and dynamic actin, *Molecular Biology of the Cell* **16** (2005), 4410–4422.

[8] B. Trinczek, M. Brajenovic, A. Ebneth and G. Drewes, MARK4 is a novel Microtubule-associated Proteins/Microtubule Affinity-regulating Kinase that bind to the cellular microtubule network and to centrosome, *Journal of Biological Chemistry* **279** (2004), 5915–5923.

[9] T. Kato, S. Satoh, H. Okabe, O. Kitahara, K. Ono, C. Kihara, T. Tanaka, T. Tsunoda, Y. Yamaoka, Y. Nakamura and Y. Furukawa, Isolation of a novel human gene, MARKL1, homologous to MARK3 and its involvement in hepatocellular carcinogenesis, *Neoplasia* **3** (2001), 4–9.

[10] A. Beghini, I. Magnani, G. Roversi, T. Piepoli, S. Di Terlizzi, R.F. Moroni, B. Pollo, A.M. Fuhrman Conti, J.K. Cowell, G. Finocchiaro and L. Larizza, The neural progenitor-restricted isoform of the MARK4 gene in 19q13.2 is upregulated in human gliomas and overexpressed in a subset of glioblastoma cell lines, *Oncogene* **22** (2003), 2581–2591.

[11] A. Schneider, R. Laage, O. von Ahsen, A. Fischer, M. Rossner, S. Scheek, S. Grünewald, R. Kuner, D. Weber, C. Krüger, B. Klaussner, B. Götz, H. Hiemisch, D. Newrzella, A. Martin-Villalba, A. Bach and M. Schwaninger, Identification of regulated genes during permanent focal cerebral ischaemia: characterization of the protein kinase 9b5/MARKL1/MARK4, *Journal of Neurochemistry* **88** (2004), 1114–1126.

[12] R.F. Moroni, S. De Biasi, P. Colapietro, L. Larizza and A. Beghini, Distinct expression pattern of microtubule-associated protein/microtubule affinity-regulating kinase 4 in differentiated neurons, *Neuroscience* **143** (2006), 83–94.

[13] L. Espinosa and E. Navarro, Human serine/threonine protein kinase EMK1: Genomic structure and cDNA cloning of isoforms produced by alternative splicing, *Cytogenetics and Cell Genetics* **81** (1998), 278–282.

[14] D.N. Louis, H. Ohgaki, O.D. Wiestler, W.K. Cavenee, P.C. Burger, A. Jouvet, B.W. Scheithauer and P. Kleihues, The 2007 WHO classification of tumours of the central nervous system, *Acta Neuropathologica* **114** (2007), 97–109.

[15] C. Hartmann, L. Johnk, G. Kitange, Y. Wu, L.K. Ashworth, R.B. Jenkins and D.N. Louis, Transcript map of the 3.7-Mb D19S112-D19S246 candidate tumor suppressor region on the long arm of chromosome 19, *Cancer Research* **62** (2002), 4100–4108.

[16] G. Roversi, R. Pfundt, R.F. Moroni, I. Magnani, S. van Reijmersdal, B. Pollo, H. Straatman, L. Larizza and E.F. Schoenmakers, Identification of novel genomic markers related to progression to glioblastoma through genomic profiling of 25 primary glioma cell lines, *Oncogene* **25** (2006), 1571–1583.

[17] I. Magnani, S. Guerneri, B. Pollo, N. Cirenei, B.M. Colombo, G. Broggi, C. Galli, O. Bugiani, S. DiDonato, G. Finocchiaro and A.M. Fuhrman-Conti, Increasing complexity of the karyotype in 50 human gliomas. Progressive evolution and de novo occurrence of cytogenetic alterations, *Cancer Genetics and Cytogenetics* **75** (1994), 77–89.

[18] J.A. Squire, S. Arab, P. Marrano, J. Bayani, J. Karaskova, M. Taylor, L. Becker, J. Rutka and M. Zielenska, Molecular cytogenetic analysis of glial tumors using spectral karyotyping and comparative genomic hybridization, *Molecular Diagnosis* **6** (2001), 93–108.

[19] S.H. Bigner, J. Mark and D.D. Bigner, Chromosomal progression of malignant human gliomas from biopsy to establishment as permanent lines in vitro, *Cancer Genetics and Cytogenetics* **24** (1987), 163–176.

[20] B.K. Hecht, C. Turc-Carel, M. Chatel, P. Grellier, J. Gioanni, R. Attias, P. Gaudray and F. Hecht, Cytogenetics of malignant gliomas: I. The autosomes with reference to rearrangements, *Cancer Genetics and Cytogenetics* **84** (1995), 1–8.

[21] P.T. Stukenberg, Triggering p53 after cytokinesis failure, *Journal of Cell Biology* **165** (2004), 607–608.

[22] G.J. Kops, B.A. Weaver and D.W. Cleveland, On the road to cancer: Aneuploidy and the mitotic checkpoint, *Nature Reviews Cancer* **5** (2005), 773–785.

[23] P. Meraldi, R. Honda and E.A. Nigg, Aurora-A overexpression reveals tetraploidization as a major route to centrosome amplification in p53-/- cells, *EMBO Journal* **21** (2002), 483–492.

[24] G. Korek, H. Martin and K. Wenzelides, A modified method for the detection of nucleolar organizer regions (AgNORs), *Acta Histochemica* **90** (1991), 155–157.

[25] C.D. Katsetos, G. Reddy, E. Dráberová, B. Smejkalová, L. Del Valle, Q. Ashraf, A. Tadevosyan, K. Yelin, T. Maraziotis, O.P. Mishra, S. Mörk, A. Legido, J. Nissanov, P.W. Baas, J.P. de Chadarévian and P. Dráber, Altered cellular distribution and subcellular sorting of gamma-tubulin in diffuse astrocytic gliomas and human glioblastoma cell lines, *Journal of Neuropathology and Experimental Neurology* **65** (2006), 465–477.

[26] G.A. Pihan, A. Purohit, J. Wallace, H. Knecht, B. Woda, P. Quesenberry and S.J. Doxsey, Centrosome defects and genetic instability in malignant tumors, *Cancer Research* **58** (1998), 3974–3985.

[27] M. Moudjou and M. Bornens, Method of centrosome isolation from cultured animal cells, in: *Cell Biology: A Laboratory Handbook*, J.E. Celis, ed., Academic Press, San Diego, CA, 1994, pp. 595–604.

[28] L.K. Chu and J.E. Sisken, The isolation and preliminary electrophoretic analysis of the mitotic spindle from cultured mammalian cells, *Experimental Cell Research* **107** (1977), 71–77.

[29] M. Muramatsu, K. Smetana and H. Busch, Quantitative aspects of isolation of nucleoli of the Walker carcinosarcoma and liver of the rat, *Cancer Research* **23** (1963), 510–518.

[30] M. Scarpelli, R. Montironi, C. Magi Galluzzi and L. Diamanti, Quantitative evaluation of nucleolar features on cytologic material in brain tumor diagnosis, *Clinical Neuropathology* **13** (1994), 323–328.

[31] A.I. Nesvizhskii, O. Vitek and R. Aebersold, Analysis and validation of proteomic data generated by tandem mass spectrometry, *Nature Methods* **4** (2007), 787–797.

[32] Y.H. Kim, J.Y. Choi, Y. Jeong, D.J. Wolgemuth and K. Rhee, Nek2 localizes to multiple sites in mitotic cells, suggesting its involvement in multiple cellular functions during the cell cycle, *Biochemical and Biophysical Research Communications* **290** (2002), 730–736.

[33] V.C. Thurston, P. Pena, R. Pestell and L.I. Binder, Nucleolar localization of the microtubule-associated protein tau in neuroblastomas using sense and anti-sense transfection strategies, *Cell Motility and the Cytoskeleton* **38** (1997), 100–110.

[34] R.R. Adams, M. Carmena and W.C. Earnshaw, Chromosomal passengers and the (aurora) ABCs of mitosis, *Trends in Cell Biology* **11** (2001), 49–54.

[35] G. Guarguaglini, P.I. Duncan, Y.D. Stierhof, T. Holmstrom, S. Duensing and E.A. Nigg, The forkhead-associated domain protein Cep170 interacts with Polo-like kinase 1 and serves as a marker for mature centrioles, *Molecular Biology of the Cell* **16** (2005), 1095–1107.

[36] M. Fabbro, B.B. Zhou, M. Takahashi, B. Sarcevic, P. Lal, M.E. Graham, B.G. Gabrielli, P.J. Robinson, E.A. Nigg, Y. Ono and K.K. Khanna, Cdk1/Erk2- and Plk1-dependent phosphorylation of a centrosome protein, Cep55, is required for its recruitment to midbody and cytokinesis, *Developmental Cell* **9** (2005), 477–488.

[37] T. Shu, H.C. Tseng, T. Sapir, P. Stern, Y. Zhou, K. Sanada, A. Fischer, F.M. Coquelle, O. Reiner and L.H. Tsai, Doublecortin-like kinase controls neurogenesis by regulating mitotic spindles and M phase progression, *Neuron* **49** (2006), 25–39.

[38] B.M. Lange, Integration of the centrosome in cell cycle control, stress response and signal transduction pathways, *Current Opinion in Cell Biology* **14** (2002), 35–43.

[39] A.R. Skop, H. Liu, J. Yates 3rd, B.J. Meyer and R. Heald, Dissection of the mammalian midbody proteome reveals conserved cytokinesis mechanisms, *Science* **305** (2004), 61–66.

[40] M. Brajenovic, G. Jobertyt, B. Küster, T. Bouwmeester and G. Drewes, Comprehensive proteomic analysis of human Par protein complexes reveals and interconnected protein network, *Journal of Biological Chemistry* **279** (2004), 12804–12811.

[41] J.P. Tassan and X. Le Goff, An overview of the KIN1/PAR-1/MARK kinase family, *Biology of the Cell* **96** (2004), 193–199.

[42] J.M. Shulman, R. Benton and D. St Johnston, The Drosophila homolog of C. Elegans PAR-1 organizes the oocyte cytoskeleton and directs oskar mRNA localization to the posterior pole, *Cell* **101** (2000), 377–388.

[43] F.M. Boisvert, S. van Koningsbruggen, J. Navascués and A.I. Lamond, The multifunctional nucleolus, *Nature Reviews Molecular Cell Biology* **8** (2007), 574–585.

[44] R.G. Weber, J.M. Bridger, A. Benner, D. Weisenberger, V. Ehemann, G. Reifenberger and P. Lichter, Centrosome amplification as a possible mechanism for numerical chromosome aberrations in cerebral primitive neuroectodermal tumors with TP53 mutations, *Cytogenetics and Cell Genetics* **83** (1998), 266–269.

[45] W.L. Lingle and J.L. Salisbury, Altered centrosome structure is associated with abnormal mitoses in human breast tumors, *American Journal of Pathology* **155** (1999), 1941–1951.

[46] J.E. Guidotti, O. Brégerie, A. Robert, P. Debey, C. Brechot and C. Desdouets, Liver cell polyploidization: a pivotal role for binuclear hepatocytes, *Journal of Biological Chemistry* **278** (2003), 19095–19101.

[47] N.J. Quintyne, J.E. Reing, D.R. Hoffelder, S.M. Gollin and W.S. Saunders, Spindle multipolarity is prevented by centrosomal clustering, *Science* **307** (2005), 127–129.

[48] B.R. Brinkley, Managing the centrosome numbers game: from chaos to stability in cancer cell division, *Trends in Cell Biology* **11** (2001), 18–21.